EPA-600/2-76-154b
July 1976

A. P. S.
ELECTRO-TUBE
EVALUATION

by

Seymour Calvert, Christian Christensen, and Charles Lake

Air Pollution Technology, Inc.
4901 Morena Boulevard, Suite 402
San Diego, California 92117

Contract No. 68-02-1496
ROAP No. 21ADL-004
Program Element No. 1AB012

EPA Project Officer: Dale L. Harmon

Industrial Environmental Research Laboratory
Office of Energy, Minerals, and Industry
Research Triangle Park, NC 27711

Prepared for

U.S. ENVIRONMENTAL PROTECTION AGENCY
Office of Research and Development
Washington, DC 20460

ABSTRACT

Fine particle collection efficiency as a function of particle size has been computed from data taken on an Air Pollution Systems, Inc. (A.P.S.) Electro-Tube.

The Electro-Tube was operated at gas flow rates of 16.9, 18.9, and 22.9 Am^3/min at ambient conditions. Titanium dioxide was generated as the test aerosol having an approximate mass mean aerodynamic diameter of 1.2 μmA with a geometric standard deviation of 2.2. Test results indicated that the overall collection efficiency was 96.9% for the high gas flow rates, 98.2% for the medium gas flow rates, and 99.3% for the low gas flow rates.

TABLE OF CONTENTS

LIST OF FIGURES

LIST OF FIGURES (Continued)

LIST OF TABLES

LIST OF ABBREVIATIONS AND SYMBOLS

Latin

d_p - particle diameter, μm

d_{pa} - aerodynamic particle diameter, μmA

d_{pc} - aerodynamic cut diameter, μmA

d_{pg} - geometric mean particle diameter, μm or μmA

d_{p50} - diameter of particle collected with 50% efficiency, μmA

Greek

μmA - aerodynamic diameter, $\mu m(g/cm^3)^{1/2}$

ρ_p - particle density, g/cm^3

σ_g - geometric standard deviation of particle size distribution

CONCLUSIONS

This evaluation was one of a series of such evaluations being conducted by the Industrial Environmental Research Laboratory of the Environmental Protection Agency to identify and test novel devices which are capable of high efficiency collection of fine particulates. The test methods used were not the usual compliance-type methods but were, rather, state-of-the-art techniques for measuring efficiency as a function of particle size using total filters, cascade impactors, and diffusion battery tests upstream and downstream from the A.P.S. Electro-Tube control device.

Experimental tests of the A.P.S. Electro-Tube were done with an aerosol of TiO_2 with a mass mean aerodynamic diameter of 1.2 μmA and a standard deviation of 2.2. Overall collection efficiencies ranged from 96.9% for high gas flow rates (22.9 Am^3/min) to 99.3% for low gas flow rates (16.9 Am^3/min).

Experimentally determined penetration for 0.5 μmA aerodynamic diameter particles was 8.6% for high gas flow, 3.7% for medium gas flow, and 1.1% for low gas flow. For 1.0 μmA aerodynamic diameter particles the penetrations were 4.3% for high gas flow, 2.27% for medium gas flow, and 0.68% for low gas flow. For 2.0 μmA aerodynamic diameter particles the penetrations were 0.22% for high gas flow, 0.39% for medium gas flow, and 0.38% for low gas flow.

The Electro-Tube performance was found to be similar to that which can be achieved in small wet electrostatic precipitators.

The A.P.S. Electro-Tube was tested using impactors with no charge neutralizers preceding them. The statically charged particles could have affected the performance of the impactors both on the outlet and the inlet sample points.

RECOMMENDATIONS

For operations where wet electrostatic precipitators are practical, the Electro-Tube should be considered as an alternative which may represent a savings in power consumption at equivalent collection efficiency.

INTRODUCTION

Air Pollution Technology, Inc. (A.P.T.), in accordance with EPA Contract No. 68-02-1496, "Experimental Tests of Novel Fine Particulate Collection Devices," conducted a performance evaluation on Air Pollution Systems, Inc. Electro-Tube system. The objective of the performance test was to determine fine particle penetration as a function of aerodynamic particle size and control device parameters.

Simultaneous inlet-outlet particle sampling measurements were taken for high, manufacturer's maximum, and two lower gas flow rates during the testing period of July 9 to 16, 1975. The maximum design flow used by A.P.S. for a twelve-inch tube was 22.9 Am^3/min.

In-stack cascade impactors, total filters, condensation nuclei counters and a portable diffusion battery were used to obtain mass loadings and size distribution data.

The results of this series of tests on the Air Pollution Systems Electro-Tube are presented in the text.

MANUFACTURER'S DESCRIPTION OF DEVICE

Air Pollution Systems has developed a two-stage electrostatic device called an "ELECTRO-TUBE" which combines a wetted wall electrostatic precipitator with hi-intensity particle precharging. The saturation charge on the particle is increased substantially from the normal 4-5 kV/cm field in a conventional precipitator to 12 kV/cm by first passing the gases through the Hi-intensity Ionizer.

The increased electrostatic charge allows a more effective migration of the fine particles in the collecting electric field of the precipitator. The collecting precipitator, a wetted wall pipe type, has a passive high-voltage electrode which emits no corona current and operates at an average applied field of 5 to 10 kV/cm. Tests have shown a high degree of stability in the electric fields up to a gas flow velocity of 6.1 m/sec (20 FPS). Despite the shorter residence time in the charging field, there is no apparent deterioration of particle charging efficiency.

A single power supply provides hi-voltage to both ionizer charger and collector sections with a total power consumption being less than 8.5 W/(m^3/min). Pressure drop through the ELECTRO-TUBE is less than 0.8 cm W.C. Since only a small amount of stack heat is transferred to the wetted walls, the ELECTRO-TUBE wet collection process does not quench the gas stream. Water utilization rate ranges between 134 and 268 liters/1000 m^3/min depending on inlet dust loading and degree of prequenching desired. The ELECTRO-TUBE is designed so that entrained water does not affect electric field stability. The unit is self demisting as any entrained water droplets are collected as fine particulate.

Installed cost for an ELECTRO-TUBE should be less than a conventional wet pipe ESP since higher flow volumes can be treated in the same size unit at higher collection efficiencies. Operating costs should be somewhat lower than a wet pipe ESP in that less electrical power is used with recycling expense and pressure drop being about the same.

SOURCE AND CONTROL SYSTEM

The pilot scale Electro-Tube of Air Pollution Systems (A.P.S.) is basically a tube electrostatic precipitator with a central rod electrode and wetted wall collector. Figure 1 is a schematic diagram of the pilot system. The inlet particles are charged in a high energy field (12 kV/cm) by a high intensity ionizer at the base of the electrode. The charged particles then migrate to the wetted wall in the body of the device in a field of 5-10 kV/cm. A.P.S. indicates that initial saturation charge on the particles is higher than the usual 4-5 kV/cm for a conventional ESP (electrostatic precipitator) and facilitates increased migration in the collecting electric field.

Under testing conditions the Electro-Tube was operated at gas flow rates of 16.9, 18.9 and 22.9 Am^3/min (596, 668, and 808 ACFM, respectively) at 20°C. Liquid flow rates could range from 1.7 to 6.4 ℓ/min according to the manufacturer's specifications, but the liquid flow was held constant at 3.8 ℓ/min during the entire test period.

The test aerosol for this study was titanium dioxide (TiO_2) which had a single particle density of 4.1 g/cm^3. The mass median aerodynamic diameter of the dispersed aerosol was about 1.2 μmA, geometric standard deviation 2.2, and agglomerate density about 3.0 g/cm^3.

Figure 2 is a schematic diagram of the particle generator used during the test which consists of a feed auger, intermediate blower, deagglomeration orifice chamber, and main blower. A cross-shaped baffle was placed at the system aerosol inlet to insure adequate mixing of the aerosol with the incoming ambient air.

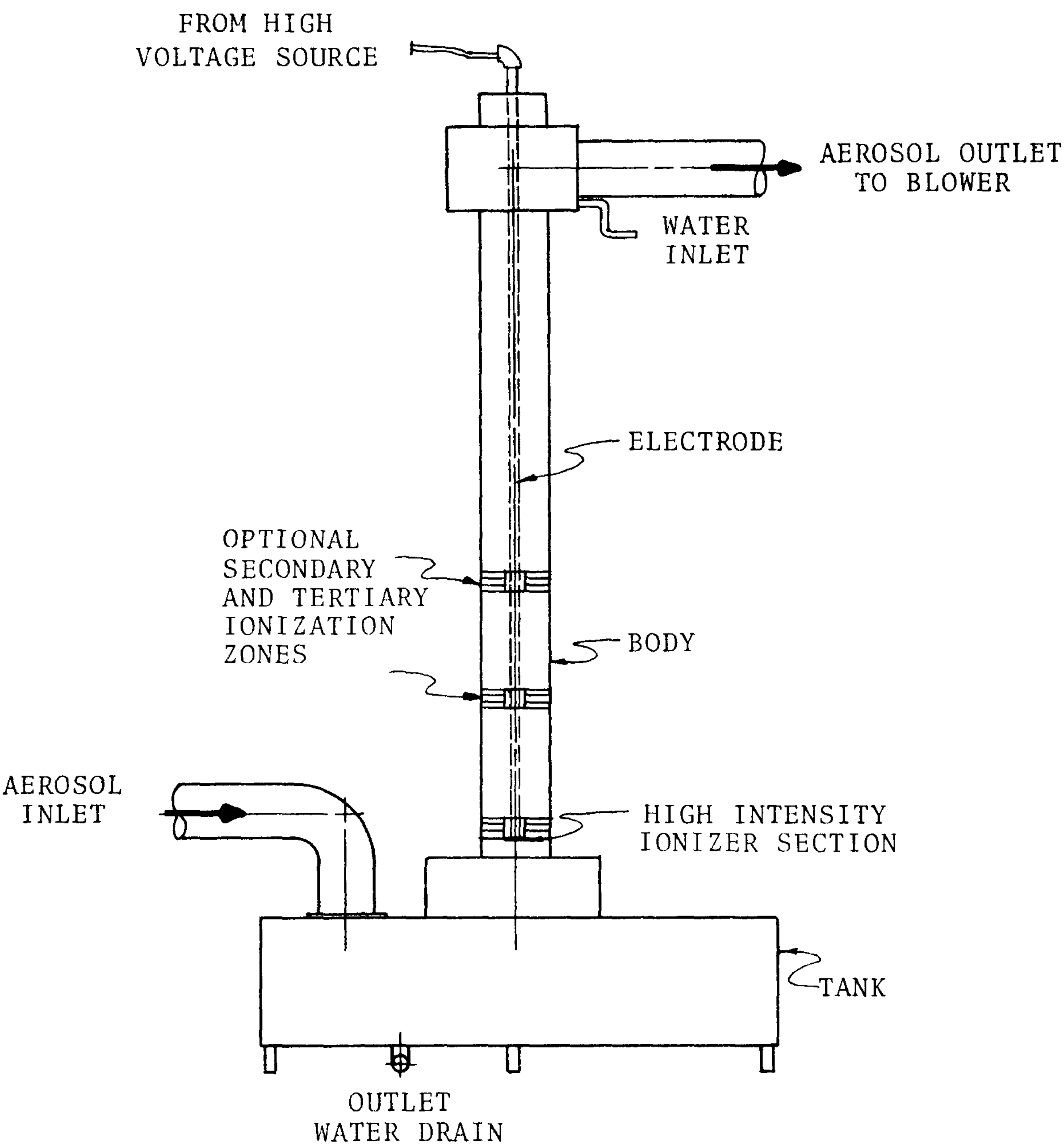

Figure 1. Diagram of A.P.S. Electro-Tube

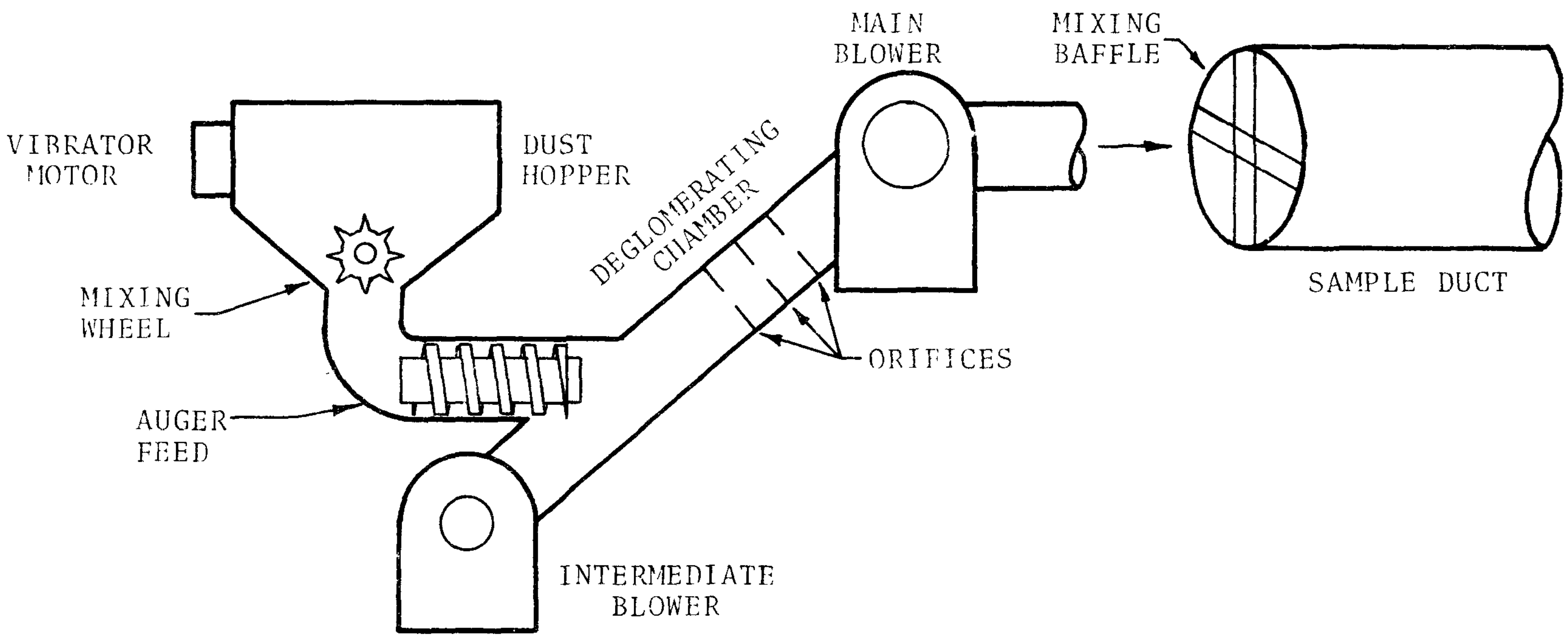

Figure 2. Schematic diagram of particle generator

TEST METHOD

The performance characteristic of the A.P.S. Electro-Tube was determined by measuring the particle size distribution and mass loadings of the inlet and outlet gas streams simultaneously.

All tests were performed using modified EPA type sampling trains with in-stack University of Washington Mark III (U.W.) cascade impactors. Figure 3 is a schematic diagram of the sample train. Greased aluminum substrates were used in the impactors to prevent particle bounce and minimize wall losses.

The Air Pollution Technology portable screen diffusion battery (A.P.T. - S.D.B.) was used for particle measurements from 0.1 μm to 0.01 μm (actual).

The A.P.T. - S.D.B. uses Brownian diffusion to accomplish the size fractionation of particles smaller than approximately 0.1 μm. Because smaller particles diffuse more readily than larger ones, successively larger particles are captured as they proceed through the battery.

Using a condensation nuclei counter (CNC) to determine the total number of particles at various points in the battery, one can obtain data which will correspond to a unique size distribution. The size distribution computation is based on calibration of the S.D.B. in the A.P.T. laboratory.

Computation of size distributions from the data on penetration is accomplished through the use of measurements of density, pressure, temperature, flow rate, and moisture, in addition to the CNC calibration factors.

During an impactor run, several inlet and outlet fine particle size measurements were taken alternately with the portable diffusion battery. Since the system

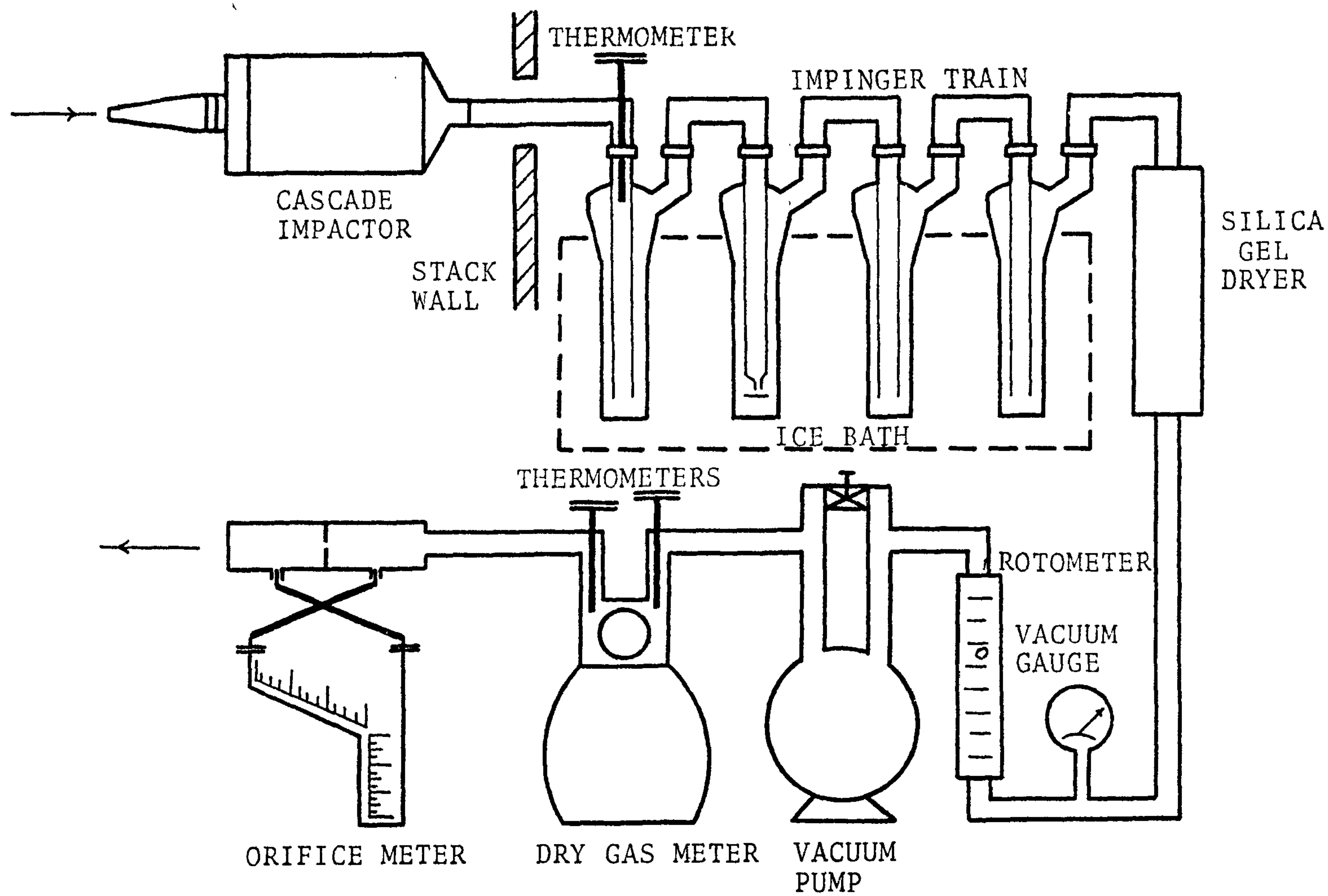

Figure 3. Modified EPA sampling train with in-stack cascade impactor

remained fairly constant during each run, alternate inlet and outlet S.D.B. measurements were considered to approximate simultaneous sampling.

In-stack filter samples were also taken to obtain total particulate loadings and overall collection efficiencies of the system.

Impactor blank runs were performed periodically to insure that the greased aluminum substrates did not react with the stack gases. A blank impactor run consisted of an impactor preceded by two glass fiber filters run at identical sample conditions as the actual sampling runs. Total filter loadings were also obtained during the blank impactor run to furnish simultaneously inlet and outlet mass concentrations and overall collection efficiency data.

Gas flow rates for all tests were determined by means of a calibrated standard-type pitot tube for velocity head measurement along with in-stack taps for continuous wet and dry bulb temperature measurements. Velocity traverses of the inlet and outlet were performed according to EPA standards and an average velocity point was selected for one point sampling. Sample flow rates were measured with the usual EPA train instruments so as to obtain isokinetic sampling.

The inlet sample port was located twelve duct diameters downstream from the dust feeder and five diameters upstream of the nearest disturbance. The outlet port was located eleven duct diameters downstream from the nearest disturbance and six diameters upstream of the blower inlet. Velocity traverses of both the inlet and the outlet gas streams revealed fully developed flow profiles.

CONDITIONS FOR RUNS

A total of nineteen simultaneous inlet and outlet sample runs was performed on the Electro-Tube. Three sets of gas flow rates were tested during the evaluation period. Diffusion battery data were taken during the last three days of testing.

Table 1, "Summary of Test Runs," is a summary of the characteristics of each test, gas flow rates and sample devices used (impactor, filter, diffusion battery). Runs 1-6, 8-9, and 18 were taken during high gas flow conditions of 22.9 Am^3/min. Runs 7, 10-14, and 17 were taken during medium gas flow conditions of 18.9 Am^3/min. Low gas flow conditions, 16.9 Am^3/min, were tested during runs 15, 16, and 19. To insure a representative dust sample, a mixing baffle was inserted at the aerosol inlet prior to run 9 and left in place for the remainder of the test period.

A power failure in the pilot plant building resulted in a loss of run 11. The cascade impactor data for run 17 were eliminated due to failure of a sample train vacuum pump while the run was under way.

Table 1. SUMMARY OF TEST RUNS

Date	Run #	Run Type	Flow, Am^3/min
7/9/75	1	Total Filter	22.9
7/9/75	2	Total Filter	22.9
7/9/75	3	Impactor	22.9
7/9/75	4	Impactor	22.9
7/10/75	5	Impactor	22.9
7/10/75	6	Total Filter	22.9
7/10/75	7	Impactor	18.9
7/10/75	8	Total Filter	22.9
7/11/75	9	Total Filter	22.9 Mixing baffle at aerosol inlet
7/11/75	10	Impactor	18.9 Mixing baffle at aerosol inlet
7/11/75	11(1)	Impactor	18.9 Mixing baffle at aerosol inlet
7/11/75	12	Impactor	18.9 Mixing baffle at aerosol inlet
7/14/75	13	Impactor	18.9 Mixing baffle at aerosol inlet
7/14/75	14	Impactor	18.9 Mixing baffle at aerosol inlet
7/14/75	15	Impactor	16.9 Mixing baffle at aerosol inlet
7/15/75	16	Impactor	16.9 Mixing baffle at aerosol inlet
7/15/75	17(2)	Impactor, DB	18.9 Mixing baffle at aerosol inlet
7/15/75	18	Impactor, DB	22.9 Mixing baffle at aerosol inlet
7/16/75	19	Impactor, DB	16.9 Mixing baffle at aerosol inlet

(1) Power failure in pilot plant building - no data obtained.
(2) Vacuum train sample pump failure - no data obtained.

OPERATING CONDITIONS

The operating conditions for the A.P.S. Electro-Tube are tabulated in Table 2 shown below:

Table 2. OPERATING CONDITIONS

Condition	Inlet	Outlet
Temperature	18-27°C	18-27°C
Velocity in Electro-Tube	4.3-5.8 m/sec (14.1-19.1 FPS)	4.4-6.0 m/sec (14.5-19.9 FPS)
Am^3/min @ 22.5°C	16.9-22.9	17.4-23.8
ACFM @ 22.5°C	596.0-808.2	615.0-841.0
DNm^3/min @ 0°C	15.4-20.9	15.9-21.7
DSCFM @ 21°C (70°F)	585.0-794.0	605.0-826.0
Vol % H_2O Vapor	1.3-2.4	1.3-2.4
Static Pressure at Sample Ports	-0.5 to -1.5 cm W.C.	-2.5 to -4.6 cm W.C.
Pressure drop across Electro-Tube: 0.53 (low flow) to 0.64 (high flow) cm W.C.		
Ionizer wall water wash rate: 3.8 ℓ/min (1 GPM)		

CASCADE IMPACTOR PARTICLE DATA

Data sets for three gas flow rates were obtained for the A.P.S. Electro-Tube. As the gas flow was fully developed one-point sample locations were used for all data points.

Table 3 is a summary of the size distribution of inlet and outlet mass loading, and overall penetration data for the various runs made. Table A-1 in the appendix summarizes the total filter loading tests while Tables A-2 to A-13 summarize inlet and outlet particle data for the impactor runs. Figures A-1 to A-12 are plots of inlet and outlet size distributions for the impactor runs. Figures A-13 to A-15 are plots of the inlet and outlet distributions for the diffusion battery data.

In this report, the symbol "d_{pa}" refers to aerodynamic diameter, which is equal to the particle diameter (d_p) in microns (μm) times the square root of the particle density (ρ_p) in grams per cubic centimeter (g/cm³) times the square root of the Cunningham slip correction factor (C'). The symbol "μmA" represents the units of aerodynamic size.

$$d_{pa} = d_p(\rho_p C')^{1/2}, \ \mu mA \qquad (1)$$

The symbol "d_{pc}" refers to the aerodynamic cut diameter or the particle diameter in which the impactor stage collection efficiency is 50%. The "d_{pc}" may also refer to the aerodynamic cut diameter of the control device in which, at the given particle diameter, the penetration is equal to 0.50. The symbol "d_{pg}" refers to the mass mean aerodynamic particle diameter for a given size distribution.

Table 3. SIZE DISTRIBUTION, MASS LOADING, AND OVERALL PENETRATION DATA*

Run No.	INLET			OUTLET			Overall Penetration (%)
	d_{pg}, μmA	σ_g	mg/DNm³	d_{pg}, μmA	σ_g	mg/DNm³	
1	Filter		177	Filter		8.7	4.9
2	Filter		242	Filter		11.0	4.6
3	1.02	2.1	185	0.69	1.4	8.5	4.6
4	1.15	2.1	248	0.71	1.5	8.7	3.5
5	1.47	2.4	571	0.70	1.5	13.0	2.3
6	Filter		775	Filter		14.5	1.9
7	1.55	2.4	1080	0.68	1.5	13.7	1.3
8	Filter		606	Filter		19.0	3.1
9	Filter		662	Filter		9.1	1.4
10	1.30	2.2	364	0.82	1.7	5.0	1.4
12	0.87	2.0	167	0.69	1.6	4.1	2.5
13	1.27	2.1	389	0.75	1.9	7.0	1.8
14	1.11	2.2	248	0.74	1.4	4.2	1.7
15	1.05	2.0	375	0.68	1.8	2.5	0.7
16	1.20	2.5	738	0.79	1.8	5.8	0.8
18	1.25	2.2	274	0.66	1.5	7.8	2.9
19	1.20	1.9	240	1.00	2.2	1.2	0.5

*d_{pg} is the geometric mass mean aerodynamic particle diameter in this table.

Isokinetic or near isokinetic sampling was undertaken for all the test runs; however, isokinetic conditions are not that crucial for sampling fine particles. For example, the error caused by sampling 4 μmA particles at a velocity 50% higher or lower than the gas stream velocity would only be about 2 or 3% of the concentration.

Single point sampling is also generally sufficient when measuring fine particle size and concentration. The fine particles will be distributed well in the gas stream, except in cases where streams with different particle concentrations have not had sufficient time to mix. To illustrate that one point sampling is sufficient for fine particles, we may note that Stokes stopping distance of a 3 μmA particle with an initial velocity of 15 m/sec (50 ft/sec) is about 0.04 cm (0.016 inches) and for a 1 μmA diameter particle is one ninth of that. Since the stopping distance is the maximum that a particle can be displaced from a gas streamline by going around a right angle bend, it becomes apparent that fine particle distribution in the gas stream will be negligibly affected by flow direction changes.

DIFFUSION BATTERY DATA

Diffusion battery data were taken during the last three days of testing. The runs were made simultaneously with cascade impactors and numbered accordingly. Runs 14 and 16 were preliminary tests to determine count and flow adjustment techniques; therefore, they were not included in the data set.

Performances during runs 17, 18, and 19 were determined by statistical conversion of inlet-outlet size distribution to cumulative number concentration and calculating the particle penetrations in the same manner as the cascade impactor analysis. Calculations were performed by a computerized FORTRAN program.

Table 4 of the text contains the size distribution summary of the diffusion battery tests. Note that the sizes given are actual rather than aerodynamic as with cascade impactor analysis. This is necessary when reducing data from the diffusion battery as the particles are evaluated in the actual size regime. Conversion to aerodynamic diameter for comparison with impactor analysis requires knowledge of the density.

The titanium dioxide powder used had a density of 4.1 g/cm^3 as measured by a pycnometer. This value agreed closely with published data for TiO_2. The solid unitary particles would have this value for their density. However, the batch of TiO_2 that was used consisted of many agglomerated as well as single particles. Most of the single particles and the detectible units of the agglomerates had diameters in the range of 0.1 to 0.3 μm as measured from scanning electron micrographs. Therefore, particles larger than about 0.3 μm were mainly agglomerates and, because of their irregular shape and possible voids, had a density less than 4.1 g/cm^3. The density of the larger particles was estimated to be about 3 g/cm^3.

Table 4. NUMBER BASIS SIZE DISTRIBUTION DATA FOR DIFFUSION BATTERY TESTS*

Run No.	INLET		OUTLET	
	d_{pg}, µm	σ_g	d_{pg}, µm	σ_g
17	0.37	7.8	0.12	7.6
18	0.14	7.2	0.035	4.3
19	0.34	7.9	0.19	7.5

*d_{pg} is the geometric number (count) mean particle diameter in this table.

Size distribution plots of diffusion battery runs have been included in Figures A-13 through A-15. The penetrations calculated from the diffusion battery data were converted to penetrations corresponding to aerodynamic diameter using both the 4.1 g/cm^3 and 3 g/cm^3 densities, and are shown in Figures 4, 5, and 6 of the next section. The lower density results in 5 to 15 percent lower particle penetrations for the three runs shown.

PARTICLE PENETRATION

The overall penetration summary is presented in Table 3. Total mass loadings were taken by cascade impactors or total filter samples. Overall penetrations tended to decrease with decreasing volumetric gas flow rates.

Average overall penetrations for the Electro-Tube were 3.1% for high flow, 1.8% for medium flow, and 0.7% for low flow. The average aerosol "d_{pg}" was 1.2 μmA with a geometric standard deviation of 2.2.

Particle penetration versus particle size were plotted for the data obtained from the Electro-Tube and appear in Figures 4-6. The data have been plotted together according to the gas flow rate of the device with diffusion battery penetration analysis included on each figure. Particle density assumptions account for discrepancies between impactor and diffusion battery penetrations.

COMPUTATION METHOD

The penetrations described above were calculated by means of a machine computation program. This method utilizes inlet and outlet particle size data which are fitted to log-normal distributions. Next the size distribution parameters and the mass concentrations are used to compute penetration as a function of particle size. Diffusion battery data yield penetration related to physical size while cascade impactor data are in terms of aerodynamic size. In order to put the results on the same basis, it is necessary to know the particle density so that one can convert physical size to aerodynamic size (or vice versa).

Particle size distribution data are conveniently represented on logarithmic probability graph paper. Often

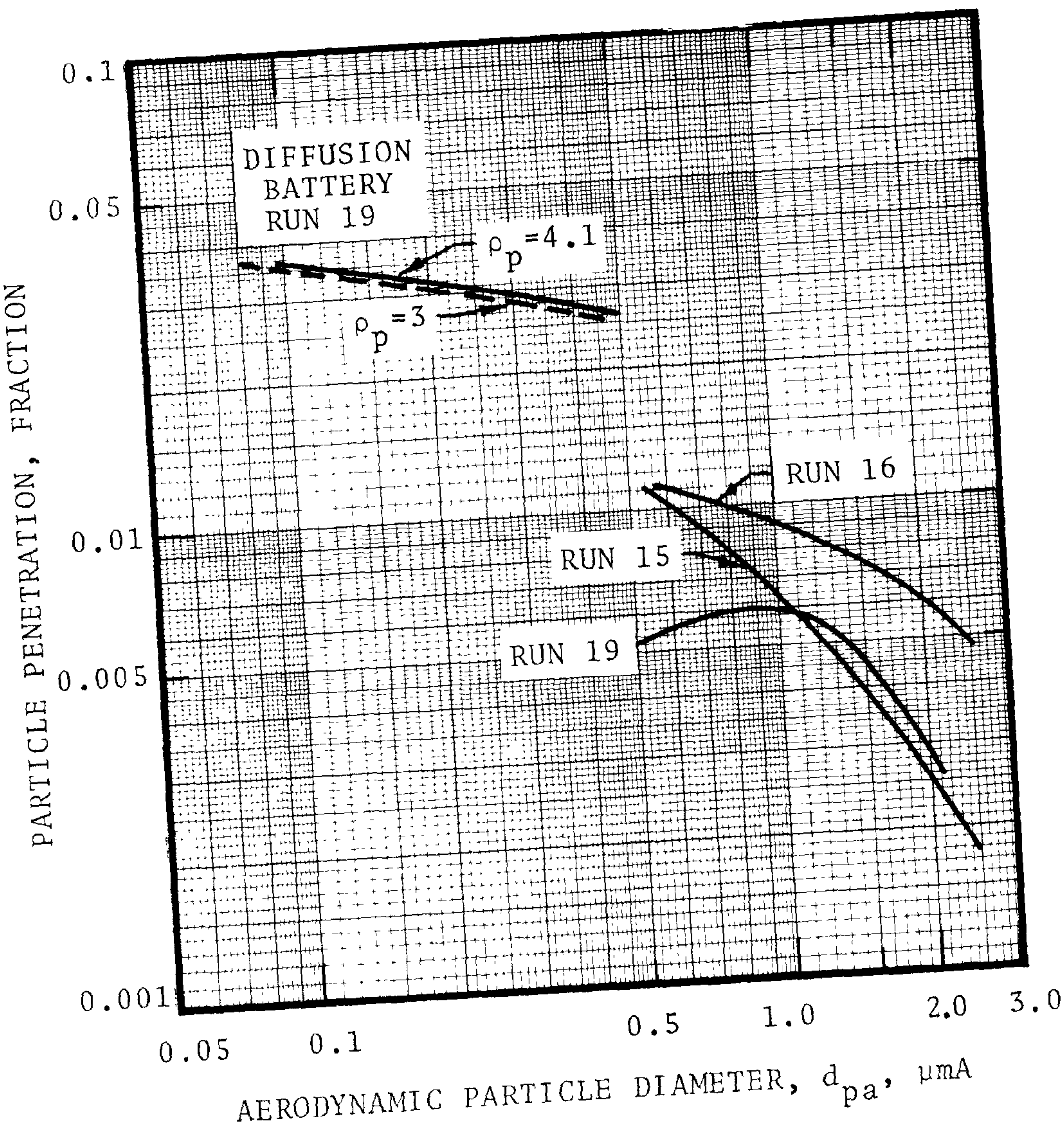

Figure 4. Penetration versus aerodynamic particle diameter for low gas flow, Runs 15, 16, 19

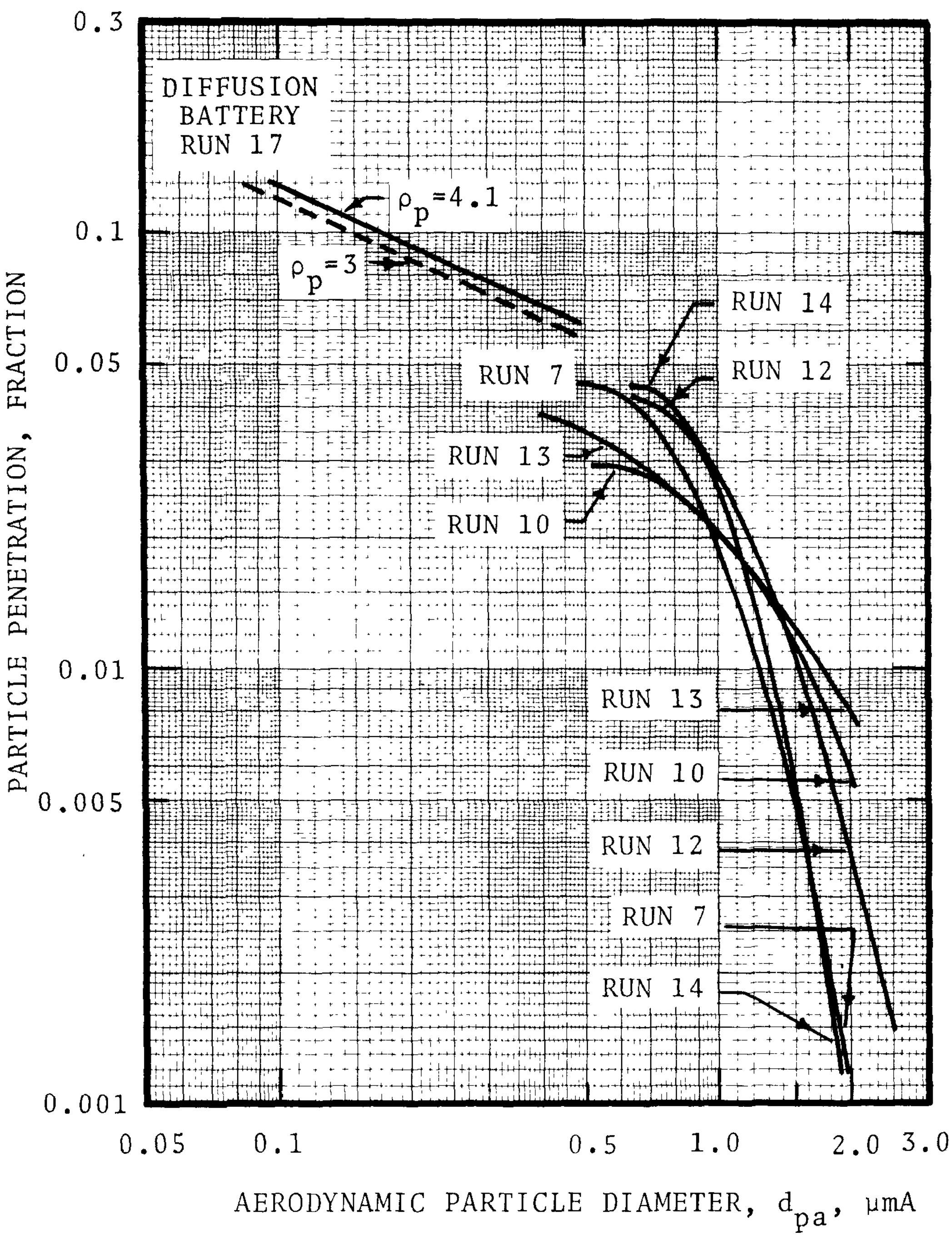

Figure 5. Penetration versus aerodynamic particle diameter for medium gas flow, Runs 7, 10, 12, 13, 14

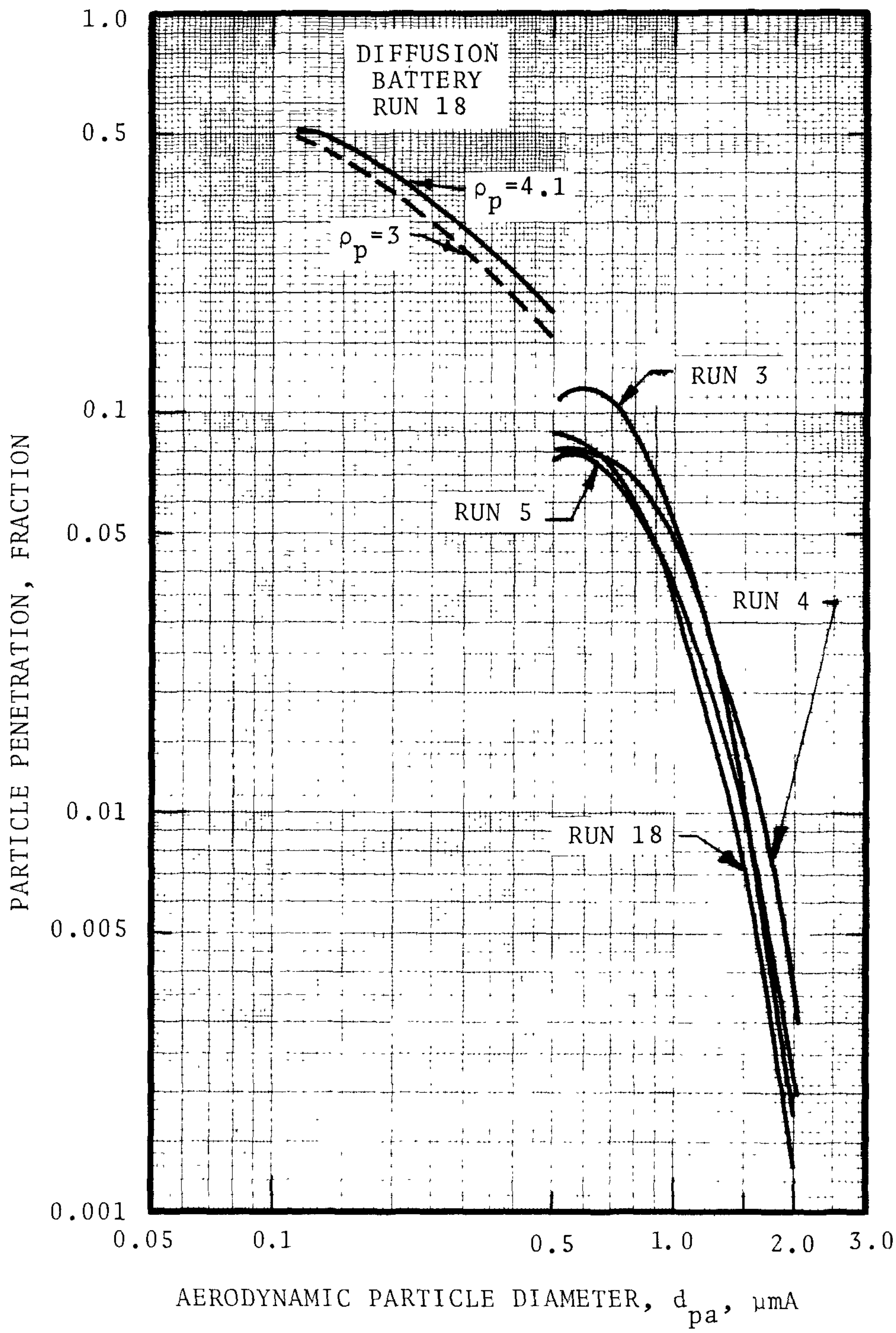

Figure 6. Penetration versus aerodynamic particle diameter for high gas flow, Runs 3, 4, 5, 18

the data fit a straight line on log-probability paper, and thus can be mathematically represented by a log-normal size distribution.

Caution must be taken when using a mathematical expression for the penetration. First, the fit of the data to a log-normal distribution must be close. Second, there is uncertainty introduced by extrapolating data beyond the size range measured. The penetration equation should not be used for particle sizes smaller or larger than those measured.

Previous calculations of penetrations have been done by manually and visually determining the ratio of the slopes of the outlet and inlet cumulative mass versus particle size curves at different particle sizes. Penetration versus particle size curves were drawn for the A.P.S. Electro-Tube by the visual method and by the machine method described above. The deviations in penetrations between the two methods were generally less than ±0.01 or 1 percent penetration.

Within limits of the particle sizes measured, the accuracy of the log-normal penetration equation depends only on how well the data fit log-normal distributions. Since the particle size data have many other inaccuracies because of the difficulties of measurement, the log-normal penetration is accurate enough, considering the ease with which it can be used. It is also most advantageous to eliminate the subjective errors possible with the visual method.

REFERENCES

Calvert, S., J. Goldshmid, D. Leith, and D. Mehta. "Scrubber Handbook," A.P.T., Inc. Riverside, California. EPA Contract No. CPA-70-95. August 1972. PB-213-016.

Calvert, S., "Engineering Design of Fine Particle Scrubbers," J. of A.P.C.A., 24, No. 10, p. 929. October 1974.

Gooch, J., J. McDonald, and S. Oglesby. "A Mathematical Model of Electrostatic Precipitators." Southern Research Institute, Birmingham, Alabama. EPA Contract No. 68-02-0265. April 1975.

Oglesby, S. and G. Nichols. "A Manual of Electrostatic Precipitator Technology." Southern Research Institute, Birmingham, Alabama. EPA Contract No. CPA 22-69-73. August 1970.

APPENDIX

APPENDIX

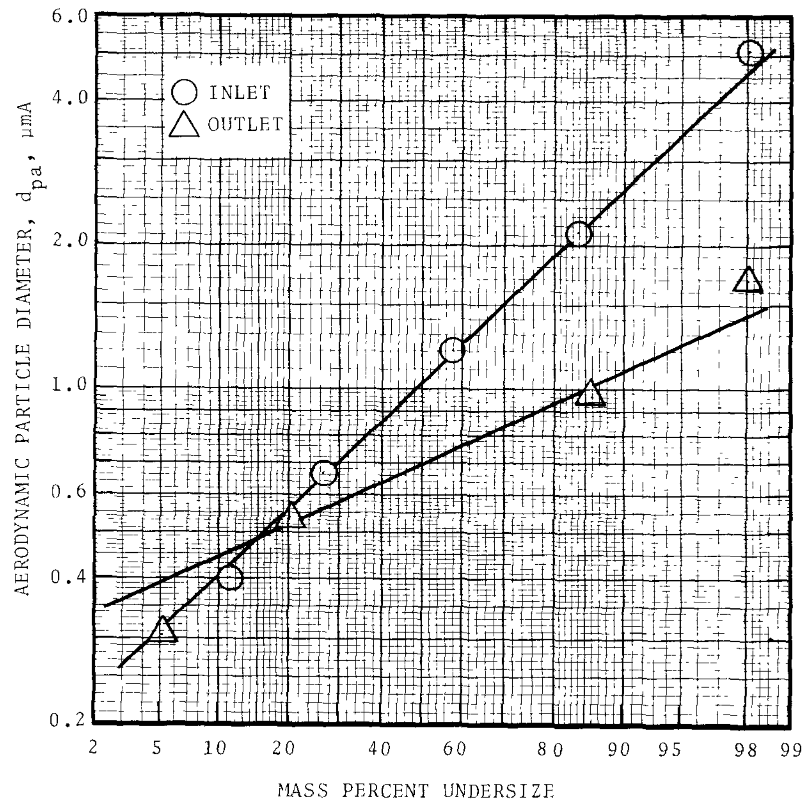

Figure A-1. Inlet and outlet size distribution for Run 3

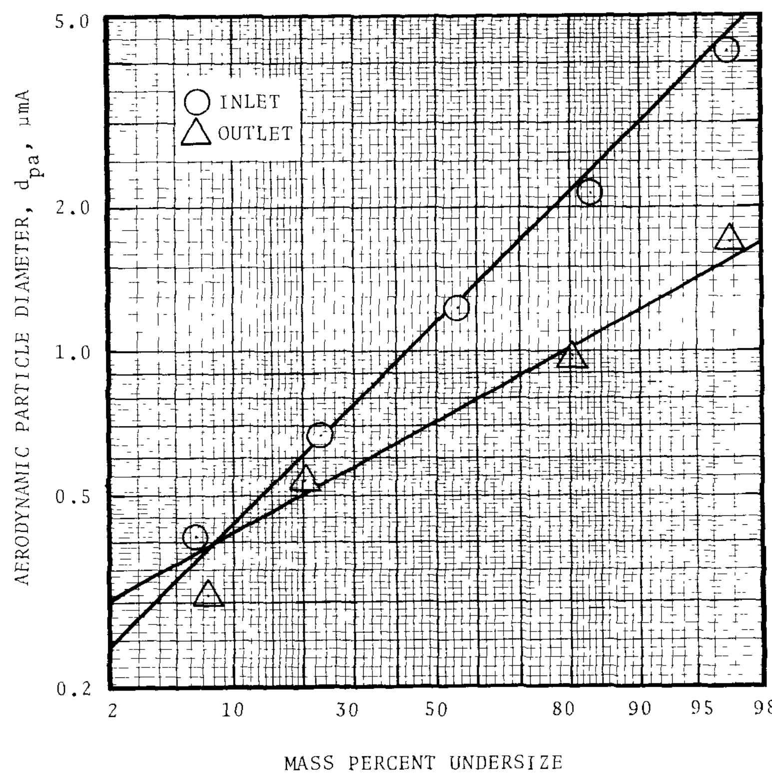

Figure A-2. Inlet and outlet size distribution for Run 4

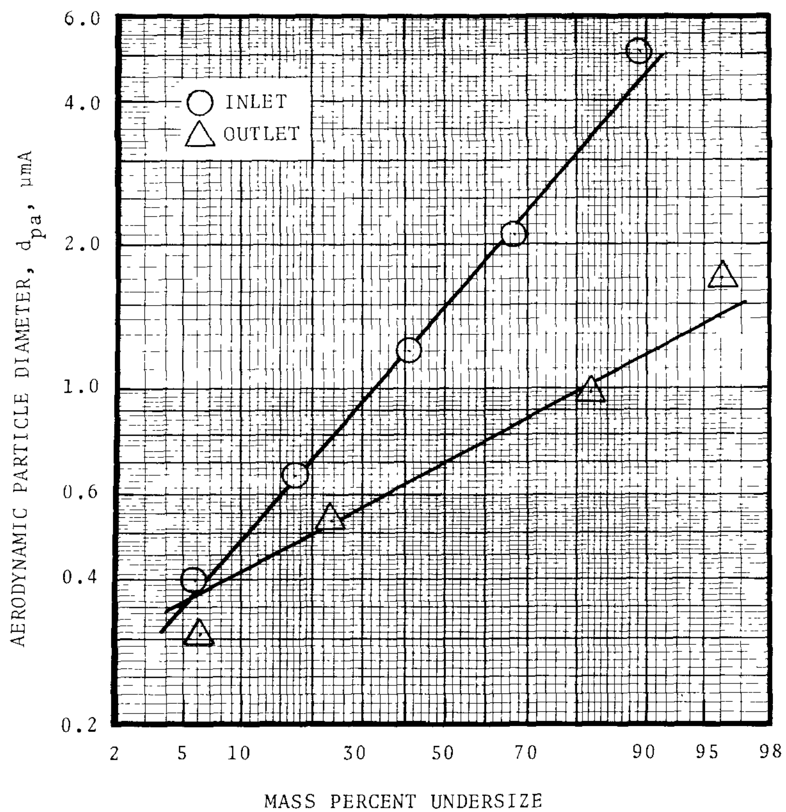

Figure A-3. Inlet and outlet size distribution for Run 5

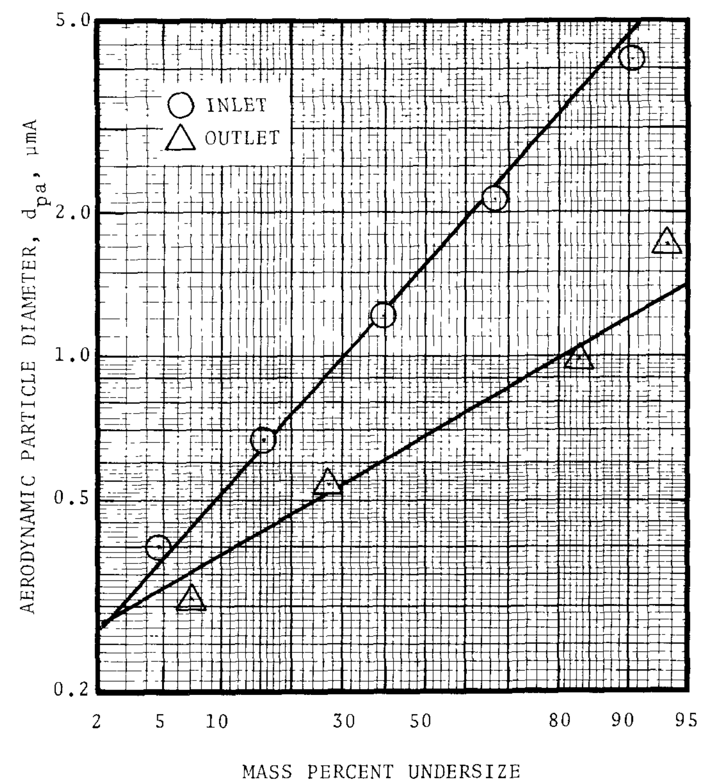

Figure A-4. Inlet and outlet size distribution for Run 7

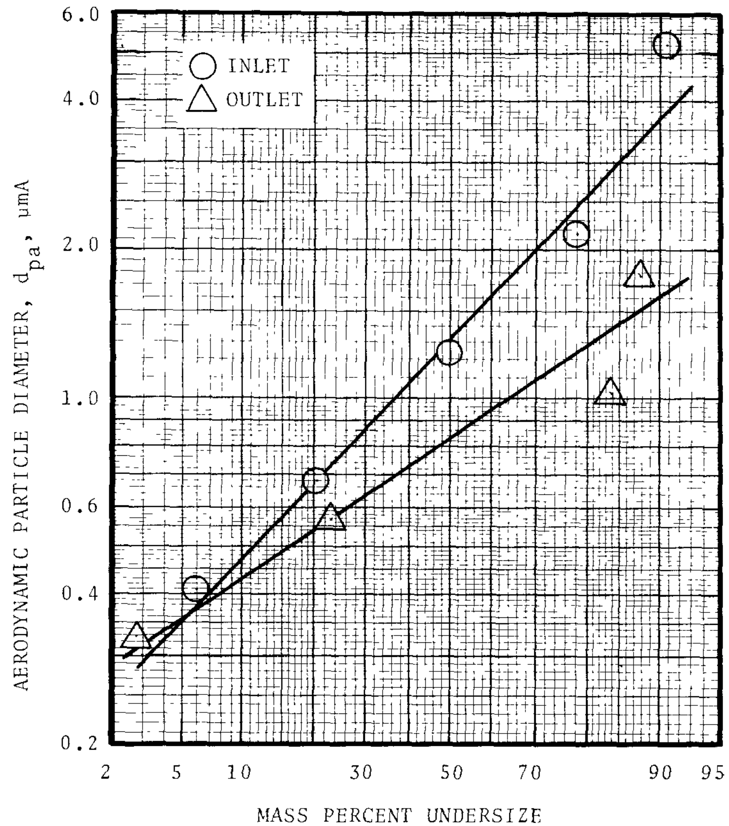

Figure A-5. Inlet and outlet size distribution for Run 10

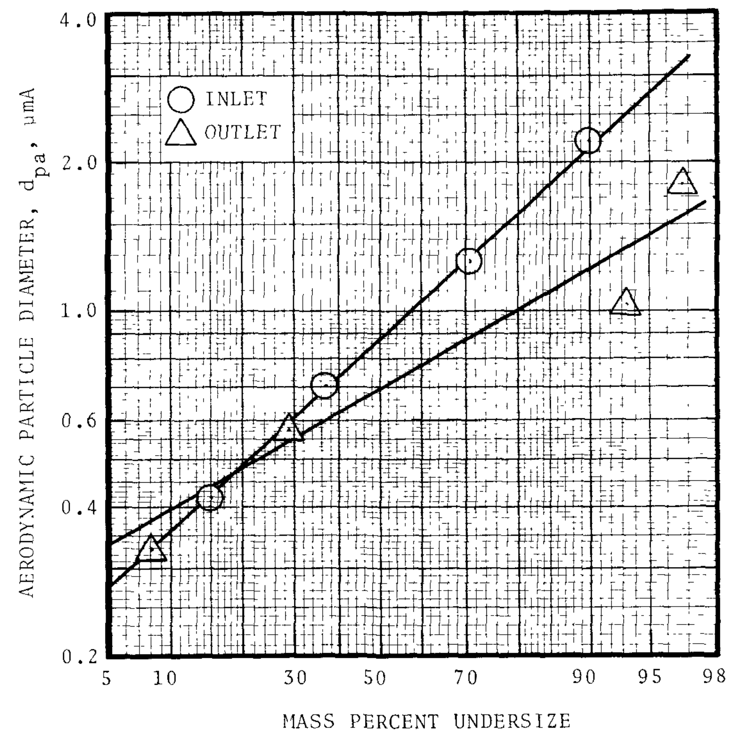

Figure A-6. Inlet and outlet size distribution for Run 12

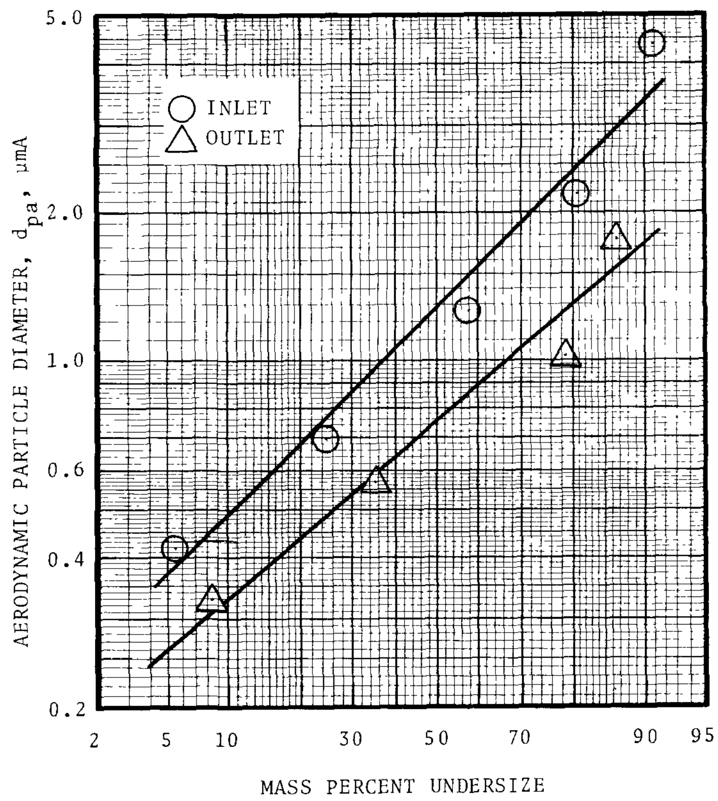

Figure A-7. Inlet and outlet size distribution for Run 13

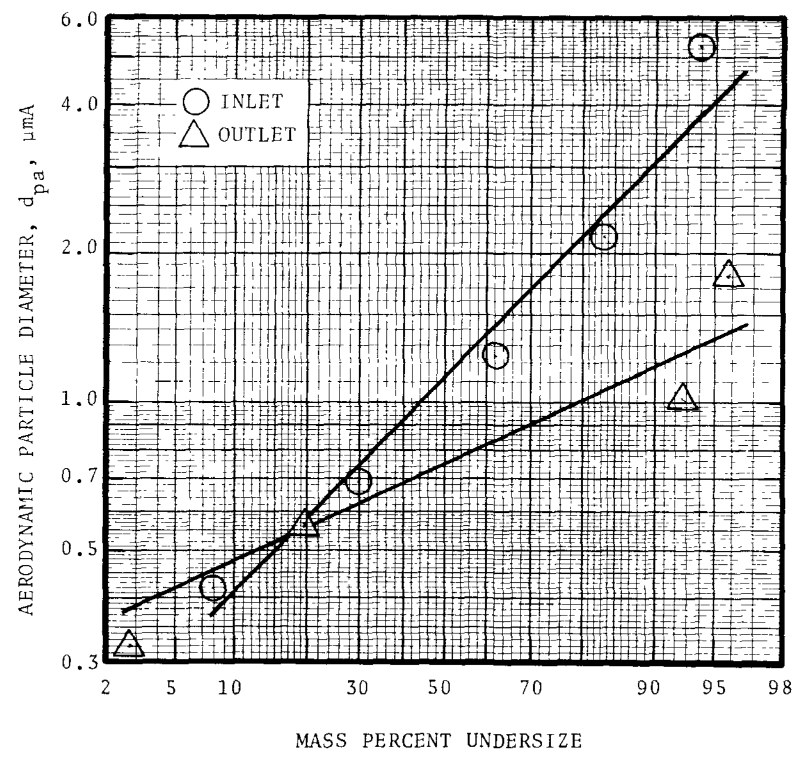

Figure A-8. Inlet and outlet size distribution for Run 14

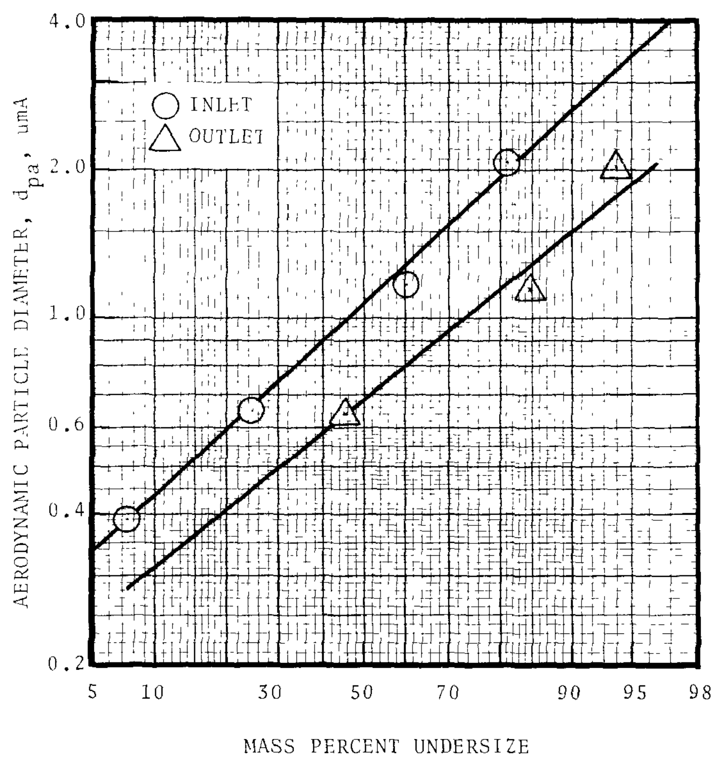

Figure A-9. Inlet and outlet size distribution for Run 15

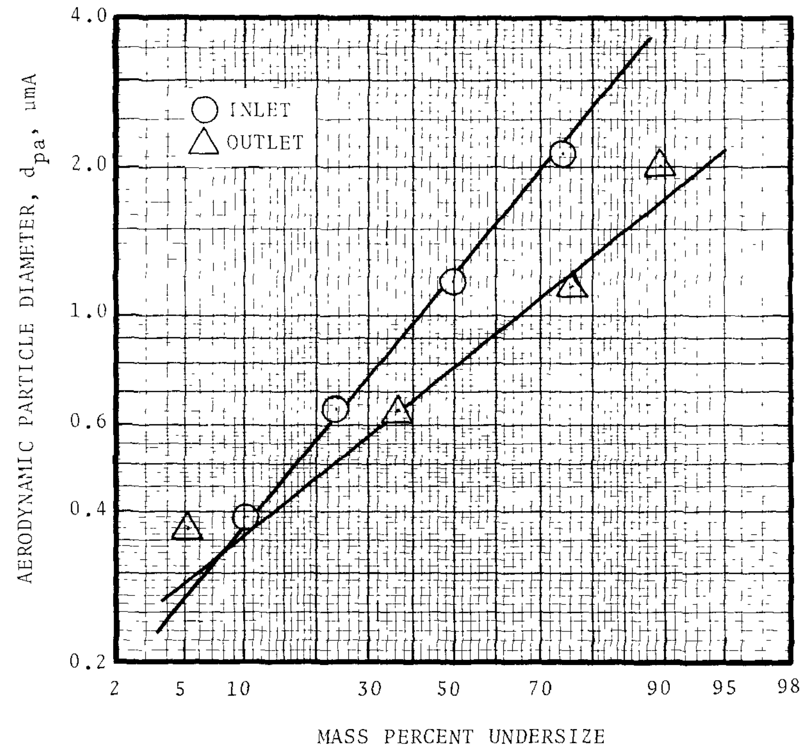

Figure A-10. Inlet and outlet size distribution for Run 16

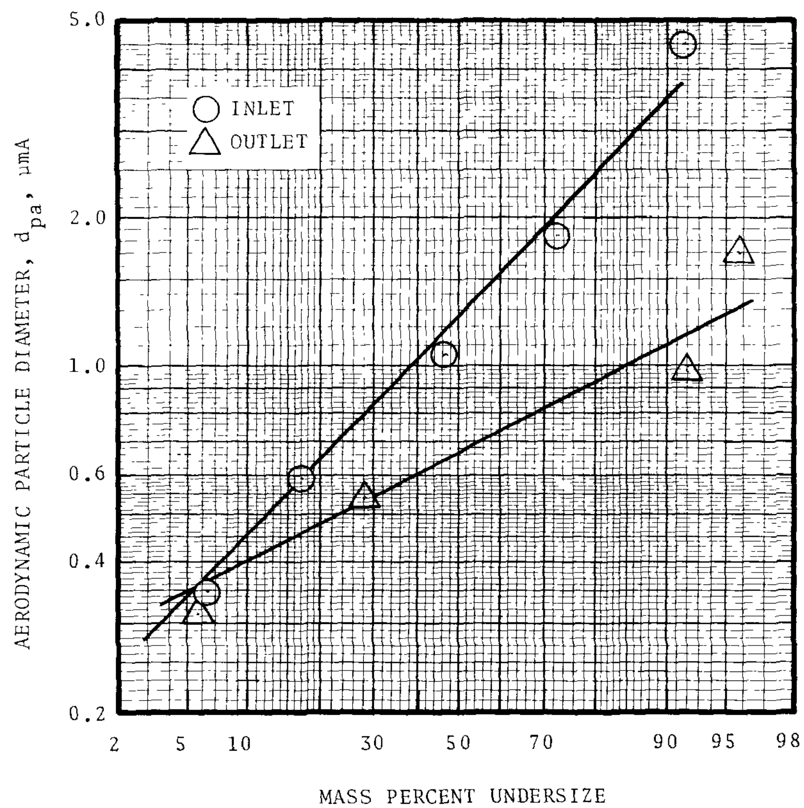

Figure A-11. Inlet and outlet size distribution for Run 18

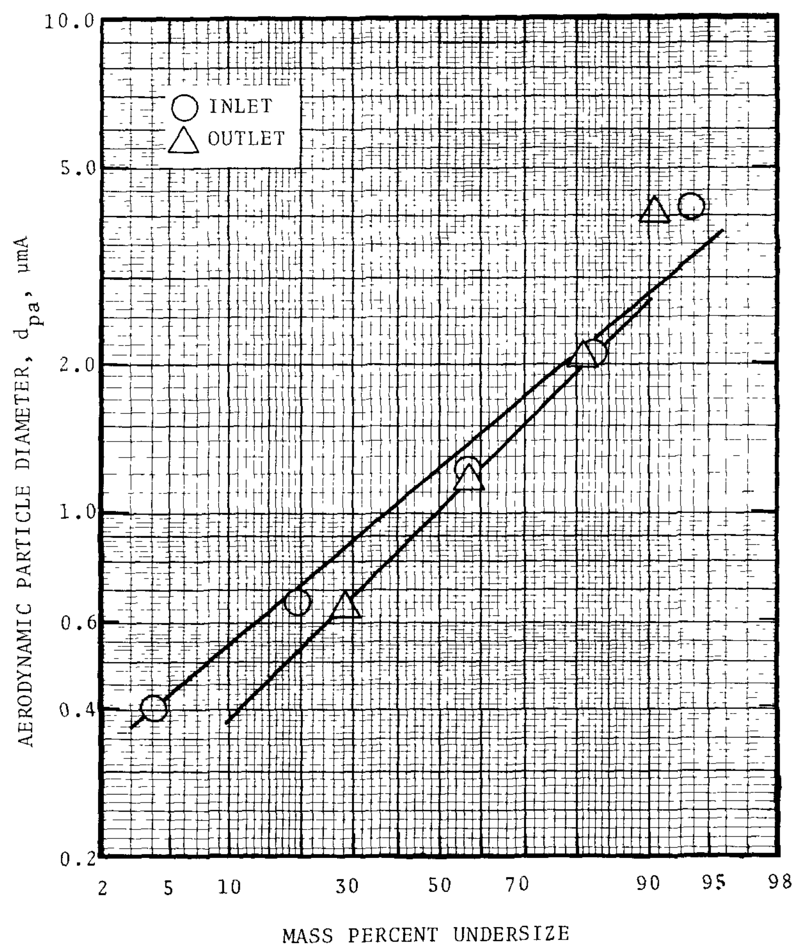

Figure A-12. Inlet and outlet size distribution for Run 19

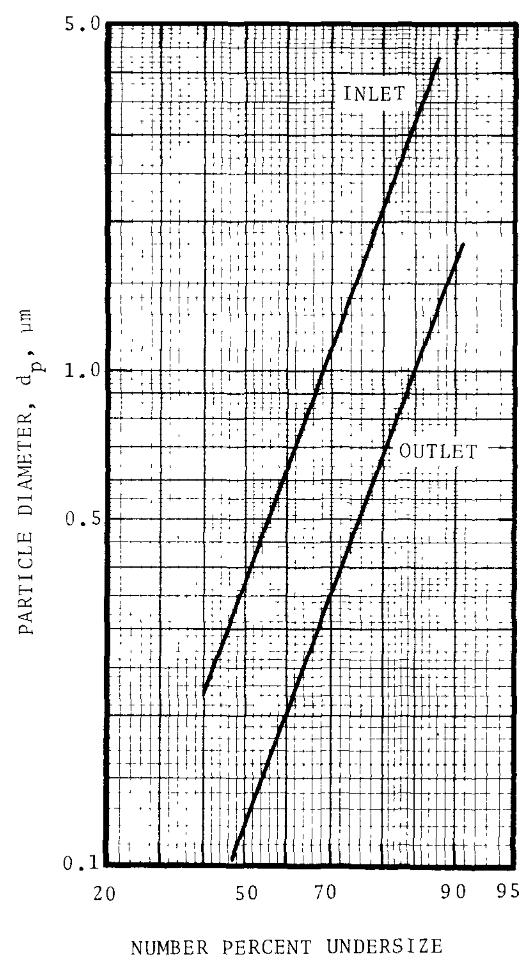

Figure A-13. Diffusion battery size distribution for inlet and outlet, Run 17

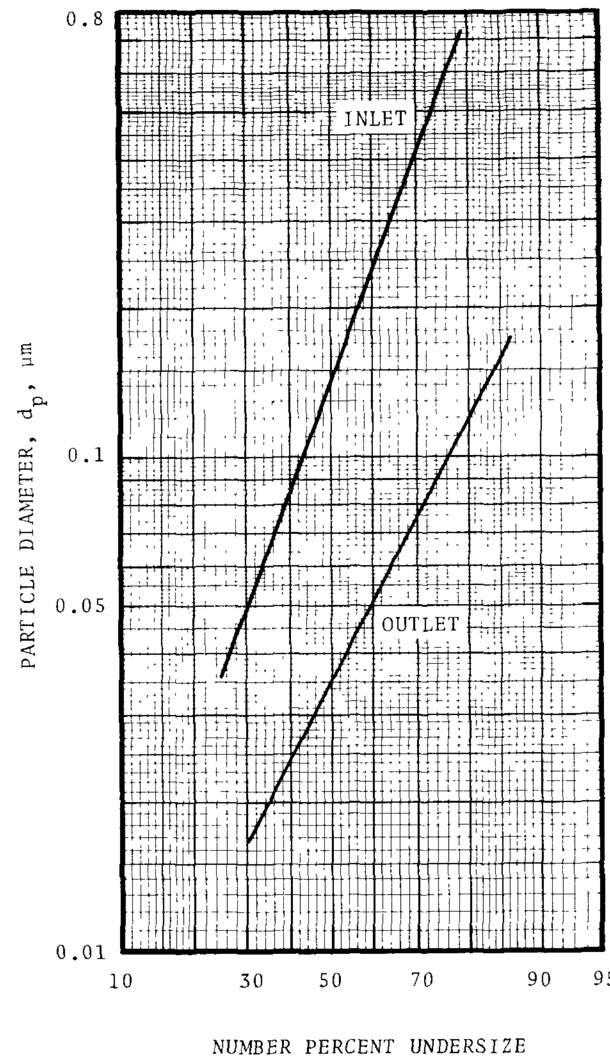

Figure A-14. Diffusion battery size distribution for inlet and outlet, Run 18

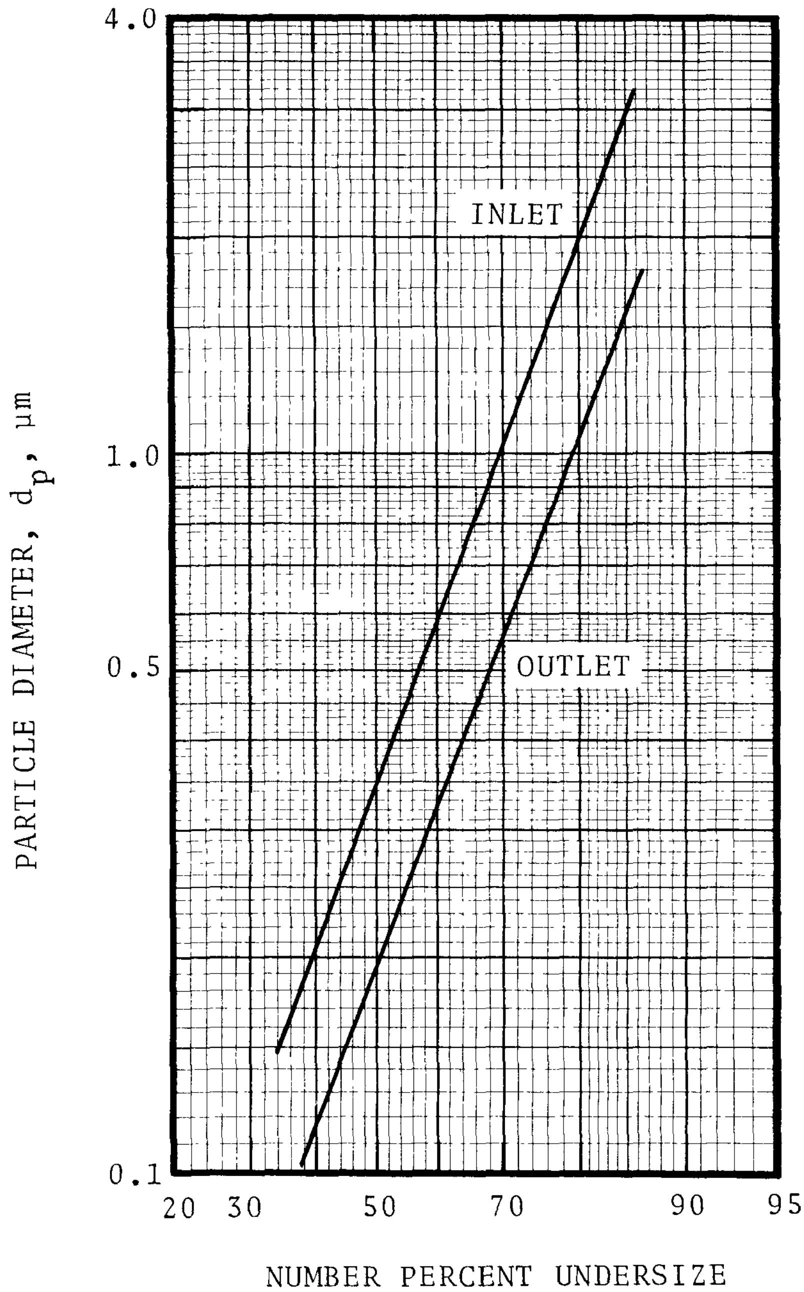

Figure A-15. Diffusion battery size distribution for inlet and outlet, Run 19